Research Article | Vol. 24, No. 19 | 5 Sep 2016 | OPTICS EXPRESS 21957
Optics EXPRESS

Attosecond pulse generation with an optimization loop in a light-field-synthesizer

B. Bódi,[1] E. Balogh,[2,3] V. Tosa,[4,6] E. Goulielmakis,[5] K. Varjú,[2,6] and P. Dombi[1,6,*]

[1]*MTA "Lendület" Ultrafast Nanooptics Group, Wigner Research Centre for Physics, 1121 Budapest, Hungary*
[2]*Department of Optics and Quantum Electronics, University of Szeged, 6720 Szeged, Hungary*
[3] *Center for Relativistic Laser Science, Institute for Basic Science (IBS), Gwangju, South Korea*
[4]*National Institute for R&D of Isotopic and Molecular Technologies, 400293 Cluj-Napoca, Romania*
[5]*Max-Planck-Institut für Quantenoptik, 85748 Garching, Germany*
[6]*ELI-ALPS, ELI-HU Nonprofit Kft., 6720 Szeged, Hungary*
[*]*dombi.peter@wigner.mta.hu*

Abstract: We developed an efficient, tailored optimization method for attopulse generation using a light-field-synthesizer [M. Hassan *et al.*, Nature **530**, 66 (2016)]. We adapted genetic optimization of single-cycle and sub-cycle waveforms to attosecond pulse generation and achieved significantly improved convergence to many target attosecond pulse shapes. Importantly, we show that the single-atom approach (based on strong field approximation) gives similar results to the more complex and numerically intensive 3D model of the attopulse generation process and that spectrally tunable attosecond pulses can be produced with a light-field synthesizer.

OCIS codes: (190.2620) Harmonic generation and mixing; (320.7110) Ultrafast nonlinear optics; (120.3180) Interferometry.

References and links

1. F. Krausz and M. Ivanov, "Attosecond physics," Rev. Mod. Phys. **81**(1), 163–234 (2009).
2. F. Calegari, G. Sansone, S. Stagira, C. Vozzi, and M. Nisoli, "Advances in attosecond science," J. Phys. At. Mol. Opt. Phys. **49**(6), 062001 (2016).
3. P. Dombi, V. S. Yakovlev, K. O'Keeffe, T. Fuji, M. Lezius, and G. Tempea, "Pulse compression with time-domain optimized chirped mirrors," Opt. Express **13**(26), 10888–10894 (2005).
4. P. Dombi, A. Apolonski, Ch. Lemell, G. G. Paulus, M. Kakehata, R. Holzwarth, T. Udem, K. Torizuka, J. Burgdörfer, T. W. Hänsch, and F. Krausz, "Direct measurement and analysis of the carrier-envelope phase in light pulses approaching the single-cycle regime," New J. Phys. **6**, 39 (2004).
5. A. Wirth, M. T. Hassan, I. Grguraš, J. Gagnon, A. Moulet, T. T. Luu, S. Pabst, R. Santra, Z. A. Alahmed, A. M. Azzeer, V. S. Yakovlev, V. Pervak, F. Krausz, and E. Goulielmakis, "Synthesized light transients," Science **334**(6053), 195–200 (2011).
6. M. T. Hassan, T. T. Luu, A. Moulet, O. Raskazovskaya, P. Zhokhov, M. Garg, N. Karpowicz, A. M. Zheltikov, V. Pervak, F. Krausz, and E. Goulielmakis, "Optical attosecond pulses and tracking the nonlinear response of bound electrons," Nature **530**(7588), 66–70 (2016).
7. M. Kitzler, K. O'Keeffe, and M. Lezius, "Attosecond control of electronic motion using light wave synthesis," J. Mod. Opt. **53**(1-2), 57–66 (2006).
8. L. Roos, M. B. Gaarde, and A. L'Huillier, "Tailoring harmonic radiation to different applications using a genetic algorithm," J. Phys. At. Mol. Opt. Phys. **34**(24), 5041–5054 (2001).
9. R. A. Bartels, M. M. Murnane, H. C. Kapteyn, I. Christov, and H. Rabitz, "Learning from learning algorithms: Application to attosecond dynamics of high-harmonic generation," Phys. Rev. A **70**(4), 043404 (2004).
10. A. B. Yedder, C. Le Bris, O. Atabek, S. Chelkowski, and A. D. Bandrauk, "Optimal control of attosecond pulse synthesis from high-order harmonic generation," Phys. Rev. A **69**(4), 041802 (2004).
11. C. Winterfeldt, C. Spielmann, and G. Gerber, "Optimal control of high-harmonic generation," Rev. Mod. Phys. **80**(1), 117–140 (2008).
12. L. E. Chipperfield, J. S. Robinson, J. W. G. Tisch, and J. P. Marangos, "Ideal waveform to generate the maximum possible electron recollision energy for any given oscillation period," Phys. Rev. Lett. **102**(6), 063003 (2009).
13. E. Balogh, B. Bódi, V. Tosa, E. Goulielmakis, K. Varju, and P. Dombi, "Genetic optimization of attosecond-pulse generation in light-field synthesizers," Phys. Rev. A **90**(2), 023855 (2014).

#263039 http://dx.doi.org/10.1364/OE.24.021957
Journal © 2016 Received 12 Apr 2016; revised 30 Jun 2016; accepted 15 Aug 2016; published 13 Sep 2016

Optics EXPRESS

14. M. Lewenstein, P. Balcou, M. Y. Ivanov, A. L'Huillier, and P. B. Corkum, "Theory of high-harmonic generation by low-frequency laser fields," Phys. Rev. A **49**(3), 2117–2132 (1994).
15. A. Moulet, V. Tosa, and E. Goulielmakis, "Coherent kiloelectronvolt x-rays generated by subcycle optical drivers: a feasibility study," Opt. Lett. **39**(21), 6189–6192 (2014).
16. E. Goulielmakis, M. Schultze, M. Hofstetter, V. S. Yakovlev, J. Gagnon, M. Uiberacker, A. L. Aquila, E. M. Gullikson, D. T. Attwood, R. Kienberger, F. Krausz, and U. Kleineberg, "Single-cycle nonlinear optics," Science **320**(5883), 1614–1617 (2008).
17. K. Zhao, Q. Zhang, M. Chini, Y. Wu, X. Wang, and Z. Chang, "Tailoring a 67 attosecond pulse through advantageous phase-mismatch," Opt. Lett. **37**(18), 3891–3893 (2012).
18. P. Tzallas, E. Skantzakis, L. A. A. Nikolopoulos, G. D. Tsakiris, and D. Charalambidis, "Extreme-ultraviolet pump-probe studies of one-femtosecond-scale electron dynamics," Nat. Phys. **7**(10), 781–784 (2011).
19. M. Suman, G. Monaco, M. G. Pelizzo, D. L. Windt, and P. Nicolosi, "Realization and characterization of an XUV multilayer coating for attosecond pulses," Opt. Express **17**(10), 7922–7932 (2009).
20. M. Hofstetter, M. Schultze, M. Fiess, B. Dennhardt, A. Guggenmos, J. Gagnon, V. S. Yakovlev, E. Goulielmakis, R. Kienberger, E. M. Gullikson, F. Krausz, and U. Kleineberg, "Attosecond dispersion control by extreme ultraviolet multilayer mirrors," Opt. Express **19**(3), 1767–1776 (2011).

1. Introduction

Attosecond pulses have become indispensable tools to investigate the fastest atomic, molecular and condensed matter processes in nature (for reviews, see [1,2]). The standard tool for achieving attopulses is high harmonic generation (HHG) of a femtosecond laser pulse. Physically, this involves the focusing of the pulse into a noble gas medium to obtain tens to some hundred harmonic orders of the fundamental radiation in a nonlinear interaction. If the fundamental is a few-cycle laser pulse [3], with stabilized carrier-envelope phase [4], the generated, suitably filtered harmonic radiation takes the form of isolated attopulses with a wide range of applications [1,2].

Requirements for femtosecond lasers driving such a typical attosecond source have been relatively standard; few-cycle pulses with ~1 mJ pulse energy were needed with stable carrier-envelope phase. A completely new perspective for controlling attopulse generation was opened recently by the demonstration of the light-field-synthesizer [5], capable of producing single, sub-cycle or even attosecond optical waveforms by synthesizing laser pulses from 3 to 4 spectral channels [5,6]. The question naturally arises, how one can control and optimize attopulse generation driven by synthesized light pulses (Fig. 1). Since a light-field-synthesizer offers a completely new mechanism for single-cycle wavepackets, HHG control is also different than in other related control schemes ([7–12] and references therein). We already demonstrated that a light-field-synthesizer can control the generation of single and double attopulses with non-trivial delays [13]. For an efficient experimental pulse shaping scheme, however, it is important that the optimization process is i) computationally fast, ii) robust and iii) predicts the generated attopulse shape with a reasonable accuracy. Here, we demonstrate a tailored optimization loop based on a genetic algorithm that is specifically adapted to analyze the single-atom (SA) response in HHG. We also analyze how the convergence of the optimization process is improved and what effect the optimization target pulse shape has on the attosecond output of this novel high scheme. The accuracy of SA response calculations is confirmed by analyzing attopulse generation with a full 3D propagation code for a set of selected driver pulses. Finally, we present the intriguing option of spectrally tunable 100-as pulse generation that can be realized with a light-field-synthesizer.

2. Modeling concept and adaptive short-pulse optimization

The quantum mechanical treatment of the HHG process involves solving the time dependent Schrödinger equation using probability matrices between the bound state through continuum and rescattering. A computationally less demanding route to calculate the time dependent dipole moment of the atomic system from first principles is to simplify the solution of the Schrödinger equation using the strong field approximation (SFA), which is valid under the conditions where high-order harmonics are usually generated [14]. Then, the dipole moment in time is given by a one-dimensional integral,

$$x(t)=i\int_{-\infty}^{t}dt'\left(\frac{\pi}{\varepsilon+i(t-t')/2}\right)^{\frac{3}{2}}d^*(p_s(t',t)-A(t))\times d(p_s(t',t)-A(t'))\,E(t')\,exp(-iS_s(t',t))+cc$$

where p_s is the stationary point of the canonical momentum, d is the atomic dipole matrix element of the bound-free transition, ε acts as an infinitesimally small positive number to avoid divergence at $t' = t$, $E(t)$ is the electric field, $A(t)$ the vector potential of the laser pulse and $S_s(t', t)$ is the quasiclassical action. Complex conjugate is represented by "*cc*". By changing the integration interval, we filtered for the short trajectories using a classical return time calculation of the cutoff. Applying Fourier transform and multiplication by ω^2 provides an approximation of the dipole radiation (i.e. HHG) spectrum. Finally, inverse Fourier transform (in a suitable spectral band) provides the shape of the attopulse(s) produced in the extreme ultraviolet (XUV) spectral domain.

This way, we can analyze the HHG process for a set of $E(t)$ fields that are generated by a light-field-synthesizer which is based on a femtosecond hollow-fiber supercontinuum [5]. The white light is split into 3 or 4 spectral channels that are separately processed and recombined (Fig. 1). Processing means optical adjustment of amplitude, delay and carrier-envelope phase in each interferometer arm in addition to compressing short pulses at the output of each channel. This way, extremely short optical wavepackets can be produced with precisely controllable waveforms. We use these waveforms for driving the HHG process. In accordance with the experimental setup [6], we took 4 spectral channels into account and adjusted their amplitude, carrier-envelope phase and relative delay. This yielded 12 free parameters for optimization, representing a broad parameter space where sophisticated numerical approaches are required. After summing up the electric fields of the channels, the driver pulse was normalized for a certain peak intensity and the SFA integral is computed, resulting in a HHG spectrum that can be spectrally filtered for further tailoring of attopulses, in line with current laboratory practice.

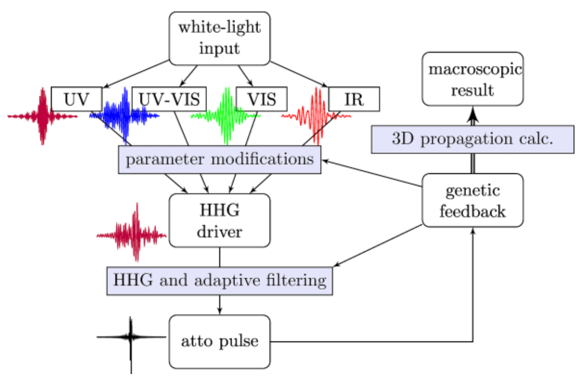

Fig. 1. Flowchart of the simulations and optimization. The colored curves show the pulses in each interferometer channel resulting in a synthesized pulse "HHG driver". Optimization is performed for the SA response, and a full 3D simulation is only performed for selected drivers.

Even though this is an interferometer with a high flexibility, the high dimensionality of the parameter space calls for tailored optimization routines. For this, we chose an evolutionary algorithm, and used it to search for a wide variety of target attopulses, including isolated and double pulses with variable, non-trivial separation as well as spectrally tunable, short attopulses. Selected results were inspected with a 3D code that accounts for macroscopic effects, like diffraction, phase-matching, dispersion and reabsorption. In this 3D model, the non-linear wave equation is solved for pulses propagating through the gas medium [15].

A crucial problem in genetic algorithms is choosing the correct fitness function to optimize for. Since in the first run we aimed at the shortest possible attopulses [16,17], it seemed natural to use the standard metric, the full width at half maximum (FWHM) as fitness parameter. However, this did not yield the shortest attopulse, as it is obvious from Fig. 2. Defining a control point at 50% of the maximum allows satellites just below this limit, and the overwhelming majority of the genetic runs converge to such solutions. However, we can generalize FWHM and search for the shortest possible full width at any arbitrary fraction of the peak. Since a short pulse length has to be kept, we defined a new fitness parameter as the product of the FWHM and the width at tenth of the peak. With this, we could remove all satellites and keep FWHM around 50 as (Fig. 2).

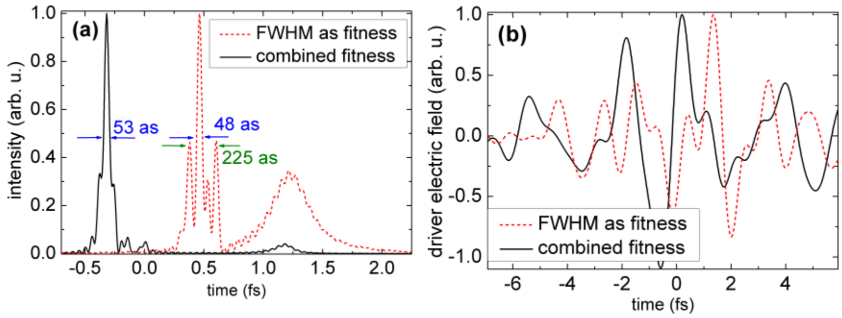

Fig. 2. Importance of fitness choice, comparing two formulas with the corresponding, optimized attopulses. **(a)** shows optimization for FWHM attopulse length (dashed) with side-pulses. However, by combining FWHM with the width at 10% of the peak, satellites are suppressed (black) without compromising pulse length. **(b)** shows the optimized driver pulse shapes for each case.

Different numerical optimization tools are used for many specific purposes, including HHG, for e.g. generating single attopulses or simulating concrete experimental schemes [7–12]. It is usually necessary to tailor the actual search algorithm for the given optimization problem in order to achieve better convergence and find global extrema with high probability. In our research, we started with a simple implementation, however, the convergence of this initial genetic algorithm was very slow, therefore, we improved its efficiency. The new version realized a balance between random scanning in many directions of the parameter space in the beginning and a fast convergence afterwards. After randomly defined individual starting points, genetic crossovers are used. These are then turned into mutations, looking for the top of the local peak. We assumed that the local extremum is within a close range of the distribution of the actual individual set and this gets more probable as the algorithm advances. Therefore, we measure the second centered moment of the population as a radius,

$$R_{pop}^2 = \sum_{n,i} \left(g(n,i) - g_0(i) \right)^2 \Big|_{\min.\, g_0(i)}$$

where $g(n,i)$ is the i^{th} normalized gene value (meaning one amplitude, phase or delay setting in the synthesizer) in the n^{th} individual of the population. $g_0(i)$ is the average of the i^{th} gene value in the given population. Using this radius, we set the next generation's mutation radius as R_{mut} = const × $R_{pop}(1 + \rho)$, where ρ is a uniform [0, 1] random value for each generation. The mutation itself uses normal distribution with the previous value as center and the mutation radius as variable. This has the advantage of adapting the step size to the population size in the parameter space. We also defined linear scaling for time delay and spectral filtering interval limits, and the time and frequency axes are discreet. The spectral amplitudes ($A_{n,i}$) are converted to gene values with $g_{amp}(n, i) = c_{amp} \log(A_{n,i})$ with suitable c_{amp} constants. To demonstrate improvements, we compared the convergence of the adapted algorithm with a standard one. Both cases progress towards the optima, but the improved algorithm does it stochastically faster (Fig. 3), approaching a local maximum in 40 generations. The standard algorithm needs more than 100 generations for most tries. Figure 3 shows also that the algorithm finds a different peak for each run, therefore, running it a few times gives more chance to find absolute extrema.

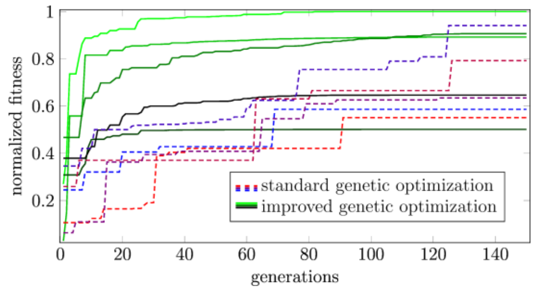

Fig. 3. Evolution towards local optima with the two different versions of the genetic code. The standard implementation of the genetic algorithm (dashed blue-red) tends to find lower fitness values in 70-130 generations than the improved one (green-black) after only 40 generations.

3. Double attopulses with non-trivial delays and 3D robustness of the model

Until this point we discussed optimizing a single attopulse only. Another direction of our investigation was about double attopulses that could be used for e.g. XUV pump-XUV probe experiments [18]. The goal was to create two short pulses of similar peak height separated by a specific non-trivial delay, i.e. a delay different from the half-cycle of the driver. This proved to be possible with even more complex driver waveforms [13]. During optimization, we need to fulfill multiple properties, such as keeping the two pulses reasonably narrow with similar peak intensities and keeping the specified delay between them. Therefore, we defined a fitness function with a versatile weighting of multiple pulse parameters. In this case, we needed more runs to reach a satisfactory result.

There is a trivial solution to generate a double attopulse with half-period delay of the fundamental. We avoided this triviality by optimizing for a wide range of different delays. Out of four different delay settings (300, 500, 700 and 900 as), the first two cases yielded double attopulses originating from different (short vs. long) trajectories. For the other two cases (700 as and 900 as), the double pulse is generated by the short trajectories, meaning that the separation happens in different half-cycles (not being obvious by looking at the driver).

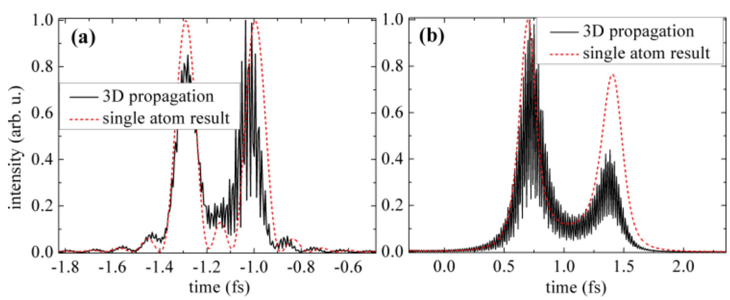

Fig. 4. Comparison of the SA optimization and full 3D propagation. Double attosecond pulses with **(a)** 300 as and **(b)** 700 as delays. Results of the SFA SA calculations (red), and the macroscopic 3D propagation in a 0.6 mm gas jet with 20 mbar pressure (black).

Finally, we examined more strictly all optimized double pulse cases by comparing it to the result of the full 3D propagation model [15]. Figure 4 compares the (genetically optimized) SA result and the macroscopic 3D modelling of double attopulses (with the same driver pulse shape). Representative, 300 as and 700 as (SA response) delays between the double pulses are shown. In these cases, the 3D propagation code produces a double pulse with 245 as and 670 as delays, respectively, both being close to the SA result. In spite of slight pulse distortions, we can conclude that under conditions where we expect good HHG efficiency, our SA model

Optics EXPRESS

gives a very good approximation of the full process. The clear double-pulse structure is easily retained with a proper choice of macroscopic properties in the 3D model (cell length, pressure and focusing), indicating the robustness of this approach. Experimentally, characterization of double pulses will be possible by attosecond streaking and any coherent XUV time structure can be probed and reconstructed with this method.

4. Efficient generation of tunable, short attosecond pulses

With the additional confirmation provided by 3D calculations, we set off to optimize the generation of tunable, short attosecond pulses with the synthesizer tool by optimizing the SA response. With a properly chosen fitness function targeting a broad HHG spectrum and a controlled spectral phase in the 90-190 eV spectral range, we managed to demonstrate the generation of widely tunable, ~100-as pulses (Fig. 5). Tunability is achieved by assuming an experimentally realistic scheme where the optimized, broad HHG spectrum is filtered by different, easily exchangable multilayer XUV mirrors having a bandwidth of some 35 eV each [19,20]. By shifting the central wavelength of the filtered radiation, we investigated the achievable attopulse shape for each spectral band. Results for 3 selected bands are shown in Fig. 5(c) with clean attopulses havng durations between 102 and 106 as.

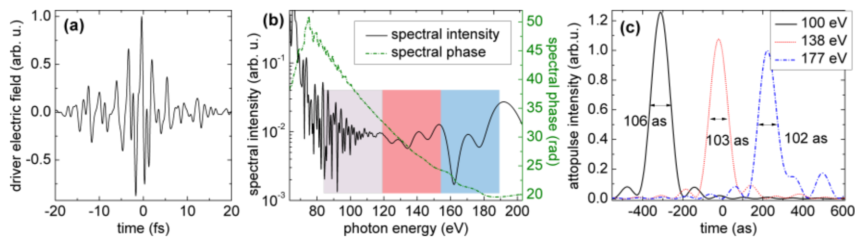

Fig. 5. Spectrally tunable attosecond pulses. **(a)** Driver electric field determined by the genetic algorithm to produce a broad quasi-continuum. **(b)** Spectrum of XUV radiation (amplitude and phase) generated by the laser field plotted in (a). Shaded regions indicate the chosen spectral ranges. **(c)** Single attosecond pulse shapes produced by filtering the XUV radiation in spectral regions that are centered at the photon energy indicated.

5. Summary

In order to study the potential of a new experimental technique, the light-field-synthesizer, we numerically implemented a genetic algorithm, and adapted it for the given physical problem (HHG). We optimized for several attosecond pulse shapes, assigning parameters of the multi-dimensional configuration space to knobs of the experimental device. We significantly improved the efficiency of the genetic algorithm for this problem. In addition, we proved that SA optimization provided similar results to that of a full 3D propagation code. This means that attopulse generation can be optimized in a computationally efficient way and experiments can be pre-optimized this way. Since attopulse characterization is experimentally intensive, one can pre-optimize drivers for particular experimental purposes (such as XUV pump – XUV probe schemes) with this method. In addition, one can utilize the light-field-synthesizer for spectrally tunable, short attosecond pulse generation with around 100 as length.

Funding

We acknowledge support by the Hungarian Academy of Sciences (“Lendület” Grant), the Partner Group Program of the Max Planck Society and the National Research, Development and Innovation Office (OTKA projects 109257 and NN107235). ELI-ALPS is supported by the European Union and co-financed by the European Regional Development Fund (GOP-1.1.1-12/B-2012-000, GINOP-2.3.6-15-2015-00001). V.T. was supported by projects PNII-ID-PCE-2012-4-0342 and PNII-RU-TE-2014-4-0425. E. G. acknowledges the European Research Council grant (Attoelectronics-258501) and the Deutsche Forschungsgemeinschaft Cluster of Excellence: Munich Centre for Advanced Photonics.